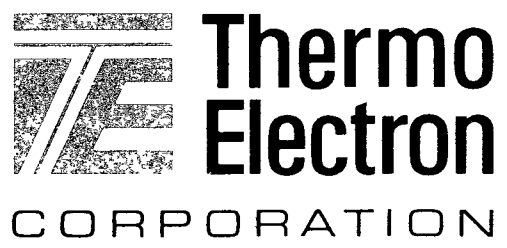


MASTER



DISCLAIMER

This report was prepared as an account of work sponsored by an agency of the United States Government. Neither the United States Government nor any agency Thereof, nor any of their employees, makes any warranty, express or implied, or assumes any legal liability or responsibility for the accuracy, completeness, or usefulness of any information, apparatus, product, or process disclosed, or represents that its use would not infringe privately owned rights. Reference herein to any specific commercial product, process, or service by trade name, trademark, manufacturer, or otherwise does not necessarily constitute or imply its endorsement, recommendation, or favoring by the United States Government or any agency thereof. The views and opinions of authors expressed herein do not necessarily state or reflect those of the United States Government or any agency thereof.

DISCLAIMER

Portions of this document may be illegible in electronic image products. Images are produced from the best available original document.

Report No. TE4258-158-82

TE--4258-158-82

DE82 010482

**DOE
ADVANCED THERMIONIC TECHNOLOGY
PROGRAM**

PROGRESS REPORT NO. 48

**July, August, September
1981**

**DOE Contract DE-AC02-81ET11201
76ET11812**

**Prepared by
Thermo Electron Corporation
101 First Avenue
Waltham, Massachusetts 02254**

DISCLAIMER

This book was prepared as an account of work sponsored by an agency of the United States Government. Neither the United States Government nor any agency thereof, nor any of their employees, makes any warranty, express or implied, or assumes any legal liability or responsibility for the accuracy, completeness, or usefulness of any information, apparatus, product, or process disclosed, or represents that its use would not infringe privately owned rights. Reference herein to any specific commercial product, process, or service by trade name, trademark, manufacturer, or otherwise does not necessarily constitute or imply its endorsement, recommendation, or favoring by the United States Government or any agency thereof. The views and opinions of authors expressed herein do not necessarily state or reflect those of the United States Government or any agency thereof.

DISTRIBUTION

0 CIRCULATED

leg

page blank

TABLE OF CONTENTS

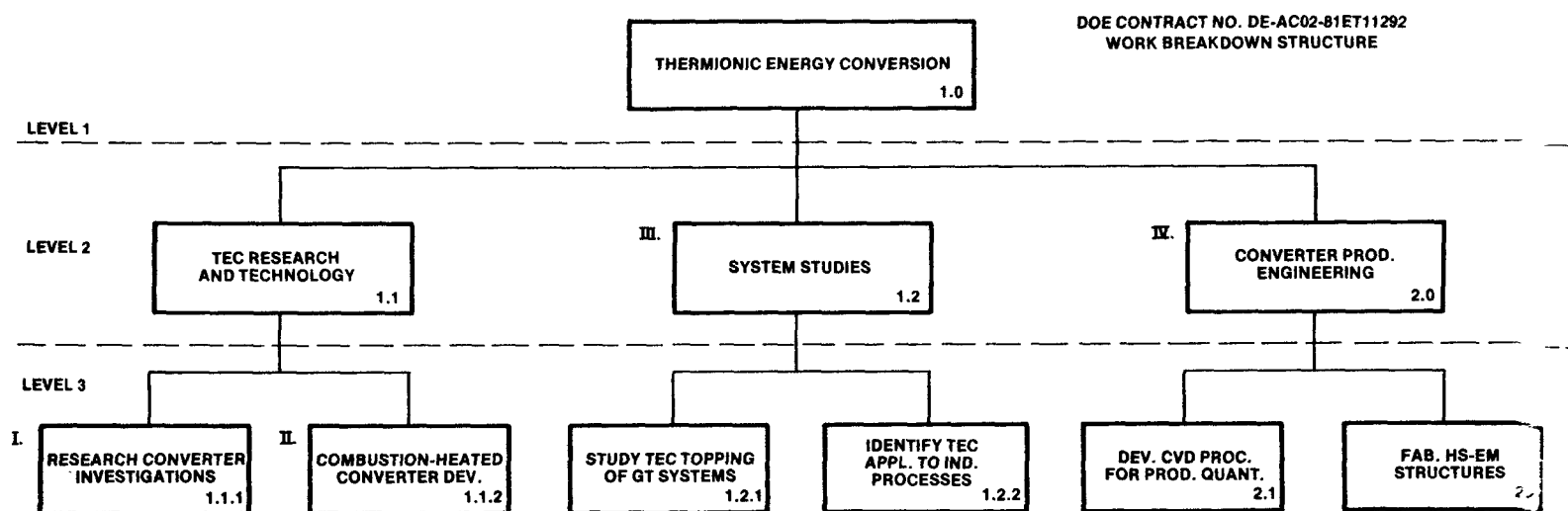
<u>Chapter</u>		<u>Page</u>
	INTRODUCTION AND SUMMARY.....	1
I.	RESEARCH CONVERTER INVESTIGATIONS	3
	A. CONVERTER NO. 268: ZrO_2 -Mo CERMET ELECTRODES.....	3
	B. CONVERTER NO. 269: TUNGSTEN EMITTER, SUBLIMED MOLYBDENUM COLLECTOR	8
	C. POSTOPERATIONAL ANALYSES	10
	1. Converter No. 262: Tungsten Emitter, Sub- limed Molybdenum Collector	10
	2. Converters Nos. 261 and 268: DFVLR Electrodes	13
II.	COMBUSTION-HEATED CONVERTER DEVELOPMENT...	19
	A. CONVERTER NO. 239: ONE-INCH DIAMETER HEMISpherical SILICON CARBIDE CONVERTER (CVD TUNGSTEN AS DEPOSITED EMITTER, NICKEL COLLECTOR).....	19
	B. CONVERTER NO. 266: TWO-INCH DIAMETER TORISpherical SILICON CARBIDE CONVERTER.	19
	C. CONVERTER NO. 270: TWO-INCH DIAMETER TORISpherical SILICON CARBIDE CONVERTER (CVD TUNGSTEN AS DEPOSITED EMITTER, SUBLIMED MOLYBDENUM COLLECTOR)	20
	D. CVD SILICON CARBIDE COATING INSIDE SINTERED MOLYBDENUM TUBE	20
III.	SYSTEM STUDIES	23
IV.	CONVERTER PRODUCTION ENGINEERING	29
V.	REFERENCES	33

INTRODUCTION AND SUMMARY

The advanced Thermionic Technology Program at Thermo Electron Corporation is sponsored by the Department of Energy (DOE). The primary long-term goal is to improve thermionic performance to the level that thermionic topping of fossil-fuel powerplants becomes technically possible and economically attractive. An intermediate goal is to operate a thermionic module in a powerplant during the mid-1980's. A short-term goal is to demonstrate reliable thermionic operation in a combustion environment.

This report covers progress made during the three-month period from July through September 1981. During this period, significant accomplishments include:

- Continuing stable output from the combustion test of the one-inch diameter hemispherical silicon carbide diode (Converter No. 239) at an emitter temperature of 1730 K for a period of over 9800 hours
- Measurement of a barrier index of 2.15 eV during the initial testing of Converter No. 266 (two-inch diameter torispherical silicon carbide diode)
- Successful thermal cycle test of a CVD silicon carbide coating inside a sintered molybdenum tube



NOTE: ROMAN NUMERALS DESIGNATE LEVEL AT WHICH TASKS ARE TO BE REPORTED

I. RESEARCH CONVERTER INVESTIGATIONS

The objective of this task is to investigate electrode pair performance as it varies with emitter and collector composition, microstructure and additives, using variable-spaced research converters heated by electron bombardment. Converter characteristics will be measured as a function of emitter temperature, collector temperature, cesium pressure, inter-electrode spacing and, if applicable, additive gas pressure.

A. CONVERTER NO. 268: ZrO_2 -Mo CERMET ELECTRODES

Converter No. 268 contains ZrO_2 cermet emitter and collector electrodes. This is the second converter built with plasma sprayed coatings from DFVLR. The technique used to form the coatings is described in References 1 and 2. The particulars of the electrodes and preoperational Auger analysis are given in Progress Report No. 46.

Results from the previous ZrO_2 -Mo cermet diode (Converter No. 261) suggested that more moderate outgassing and operating temperatures should give improved results. Prior to cesiation, the emitter and collector were outgassed to 1450 and 760 K, respectively. Initial performance measurements were made at an emitter temperature of 1400 K.

A cesium family at $T_E = 1400$ K, and $d = 0.5$ mm is shown in Figure 1. In contrast to the previous diode, this output was stable and reproducible. Figure 2 shows the optimum performance at $T_E = 1400$ K, parametric in interelectrode spacing. At a current density of 5 A/cm^2 , the barrier index was 2.00 eV at this emitter temperature. After 150 hours of stable operation, the performance was measured at emitter temperatures of 1500 and 1600 K. Figure 3 shows a cesium reservoir temperature family at $T_E = 1500$ K, $T_C = 800$ K, and $d = 0.5$ mm. The barrier index at 5 A/cm^2 at these conditions was 2.08 eV. Again, the emitter temperature was raised 100 degrees. At these conditions, the barrier index was 2.30 eV at 5 A/cm^2 . These results are given in Figure 4. As is apparent from this figure, the output degraded significantly. This degradation appeared

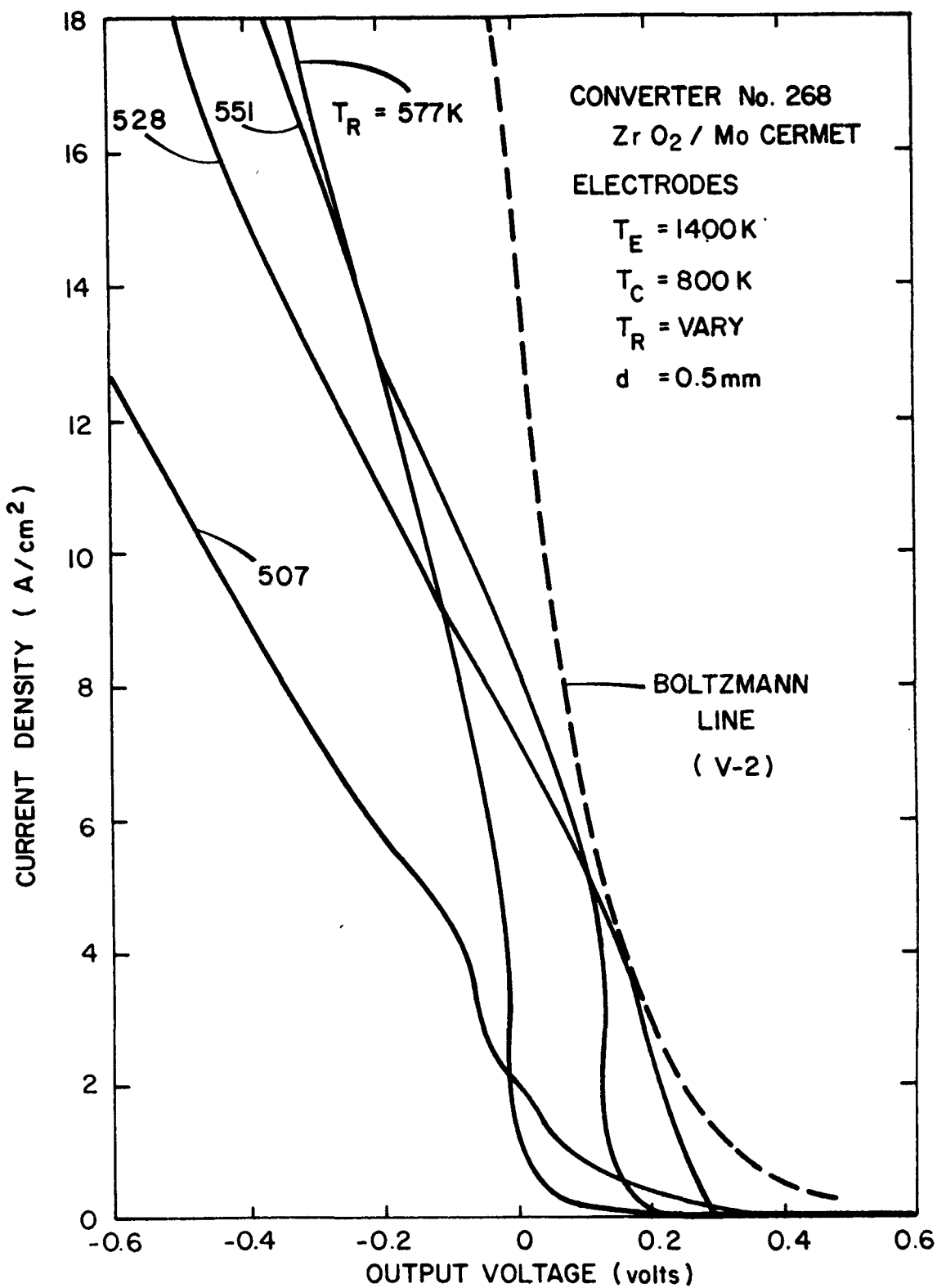


Figure 1. Cesium Reservoir Temperature Family at $T_E = 1400 K$,
 $T_C = 800 K$, and $d = 0.50 mm$ for Converter No. 268

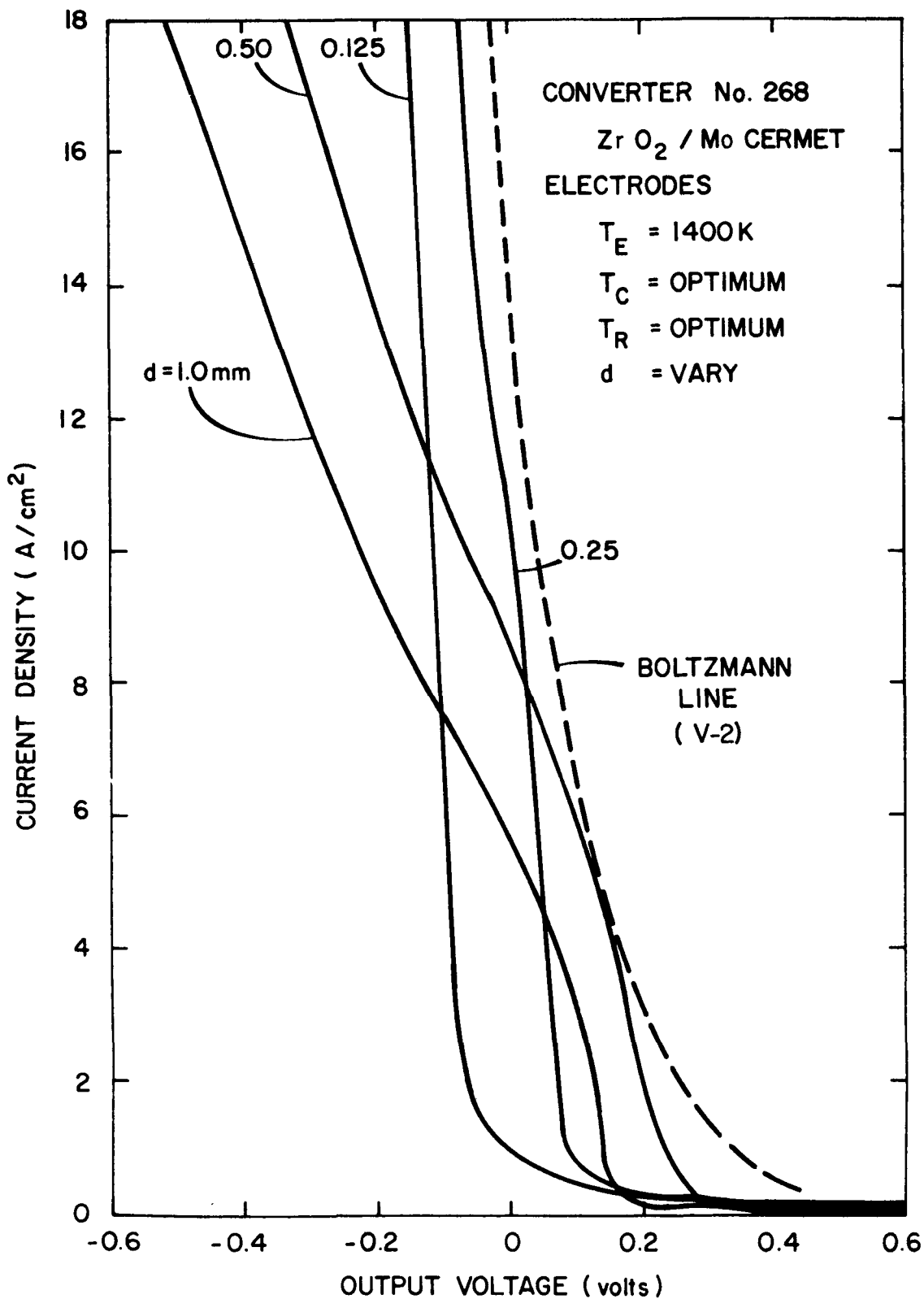


Figure 2. Optimized Converter Performance at $T_E = 1400$ K and Various Interelectrode Spacings for Converter No. 268

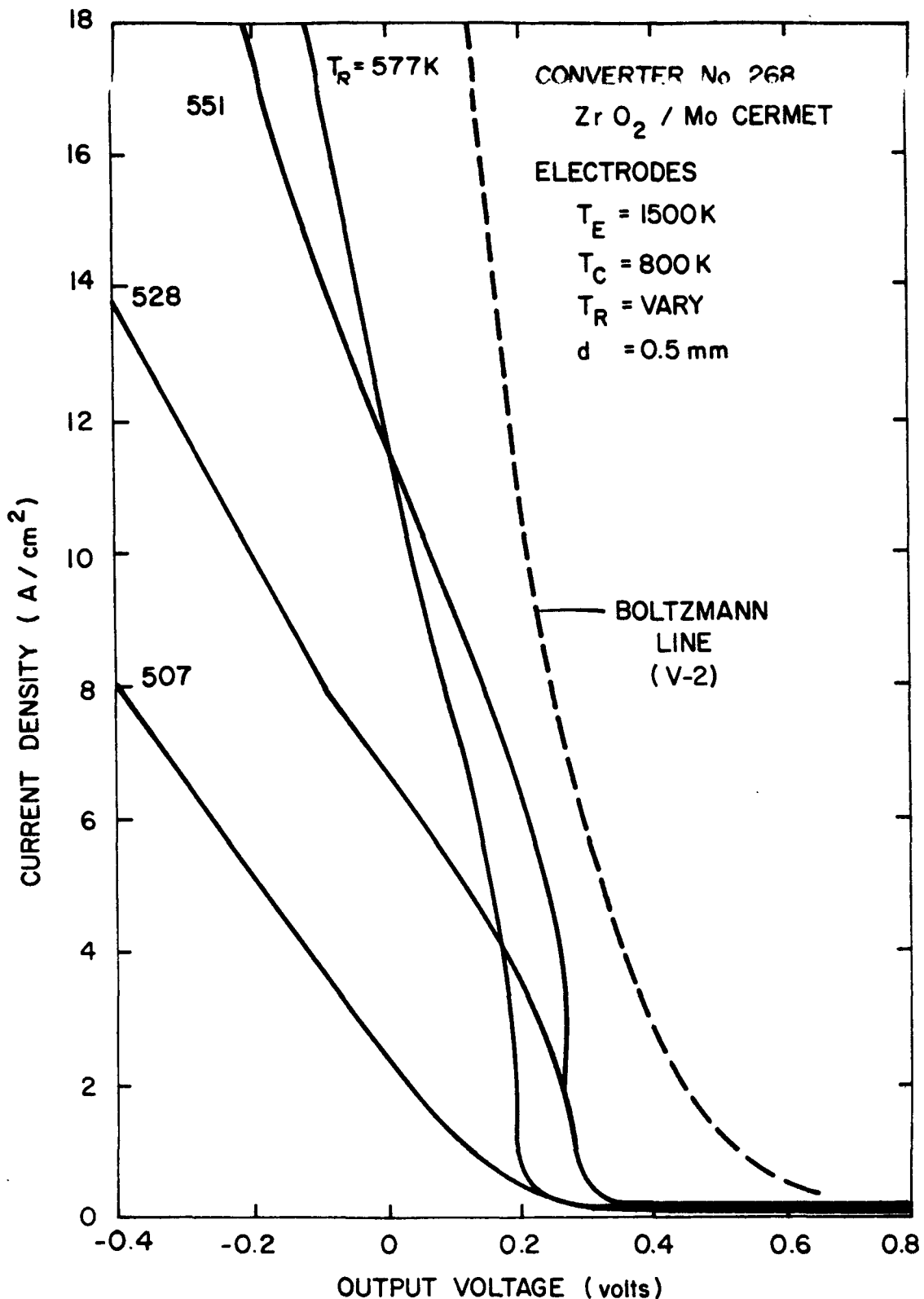


Figure 3. Cesium Reservoir Temperature Family at $T_E = 1500 K$, $T_C = 800 K$, and $d = 0.5 mm$ for Converter No. 268

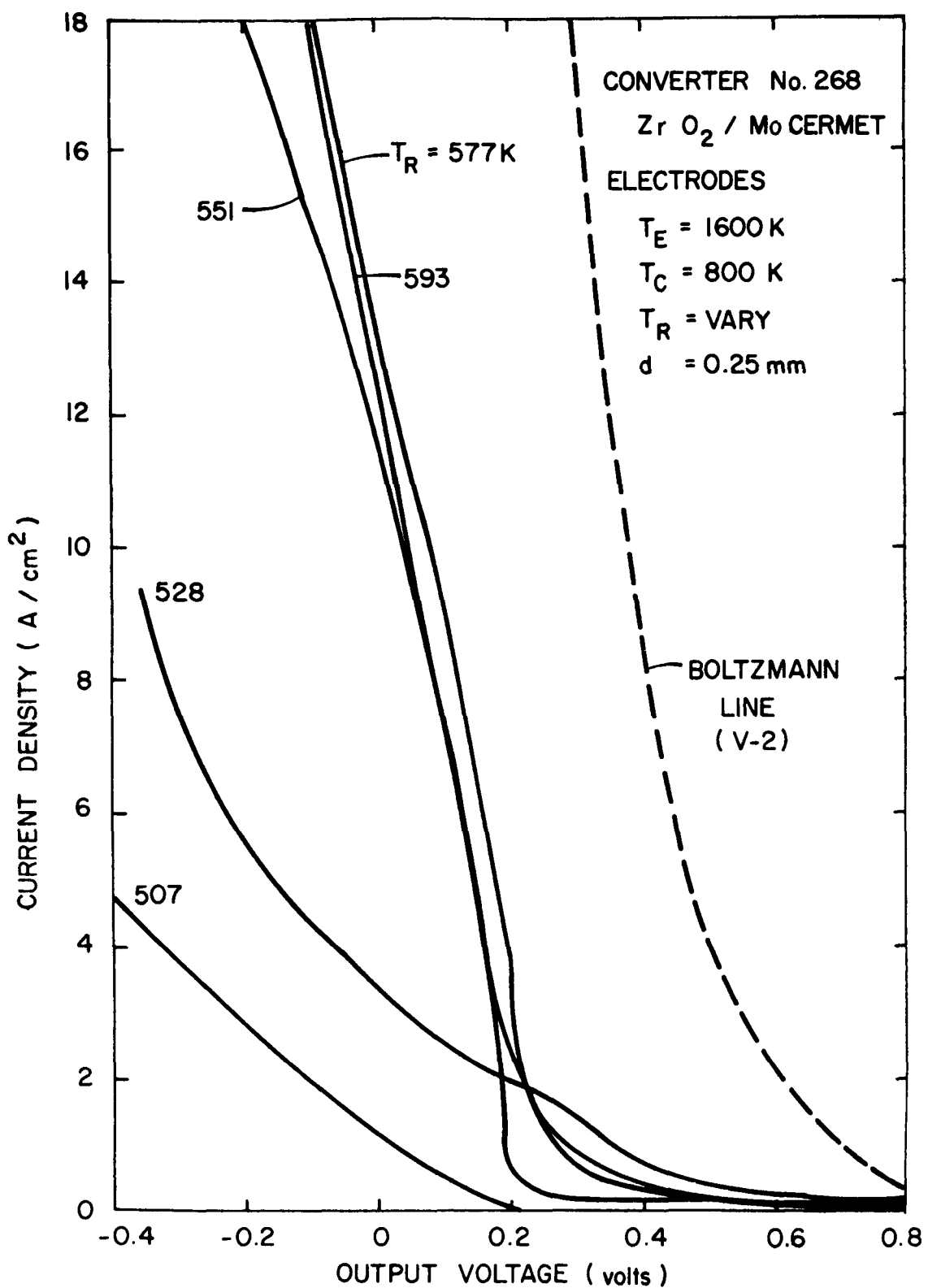


Figure 4. Cesium Reservoir Temperature Family at $T_E = 1600$ K,
 $T_C = 800$ K, and $d = 0.25$ mm for Converter No. 268

to be irreversible. Upon returning to an emitter temperature of 1400 K the barrier index was greater than 2.30 eV, compared to the 2.00 eV recorded previously.

At this point, the diode was taken off test and opened for post-operational diagnostics. These results are discussed in Section I-C.2 of this report.

B. CONVERTER NO. 269: TUNGSTEN EMITTER, SUBLIMED MOLYBDENUM COLLECTOR

The collector for Converter No. 269 was made by subliming molybdenum in the presence of oxygen onto a nickel substrate. This coating contained 17,000 ppm of oxygen by weight. The diode was made to further investigate the behavior of sublimed molybdenum coatings on nickel.

Although the performance was not spectacular, the diode progressed through the qualitative changes associated with sublimed molybdenum collectors. Within a very brief period, the current density at an output potential of 0.4 V increased from 2.0 to 6.0 A/cm². A cesium reservoir temperature family at $T_E = 1650$ K, $T_C = 800$ K, and $d = 1.00$ mm is shown in Figure 5. The barrier index was 2.12 eV at 5 A/cm².

After approximately 20 hours of stable operation, the output power degraded. The barrier index increased to 2.30 eV and the J-V characteristics became insensitive to collector temperature. This behavior was similar to that of Converter No. 262, which was tested during the last reporting period (Progress Report No. 47). The output of Converter No. 262 remained stable for a period of 900 hours.

At approximately the 900 hour mark, the output power slowly improved to its best performance of $V_B = 2.12$ eV. The J-V characteristics at this point were virtually indistinguishable from those shown in Figure 5. After this output remained stable for 100 hours, the diode was taken off test and opened for postoperational diagnosis.

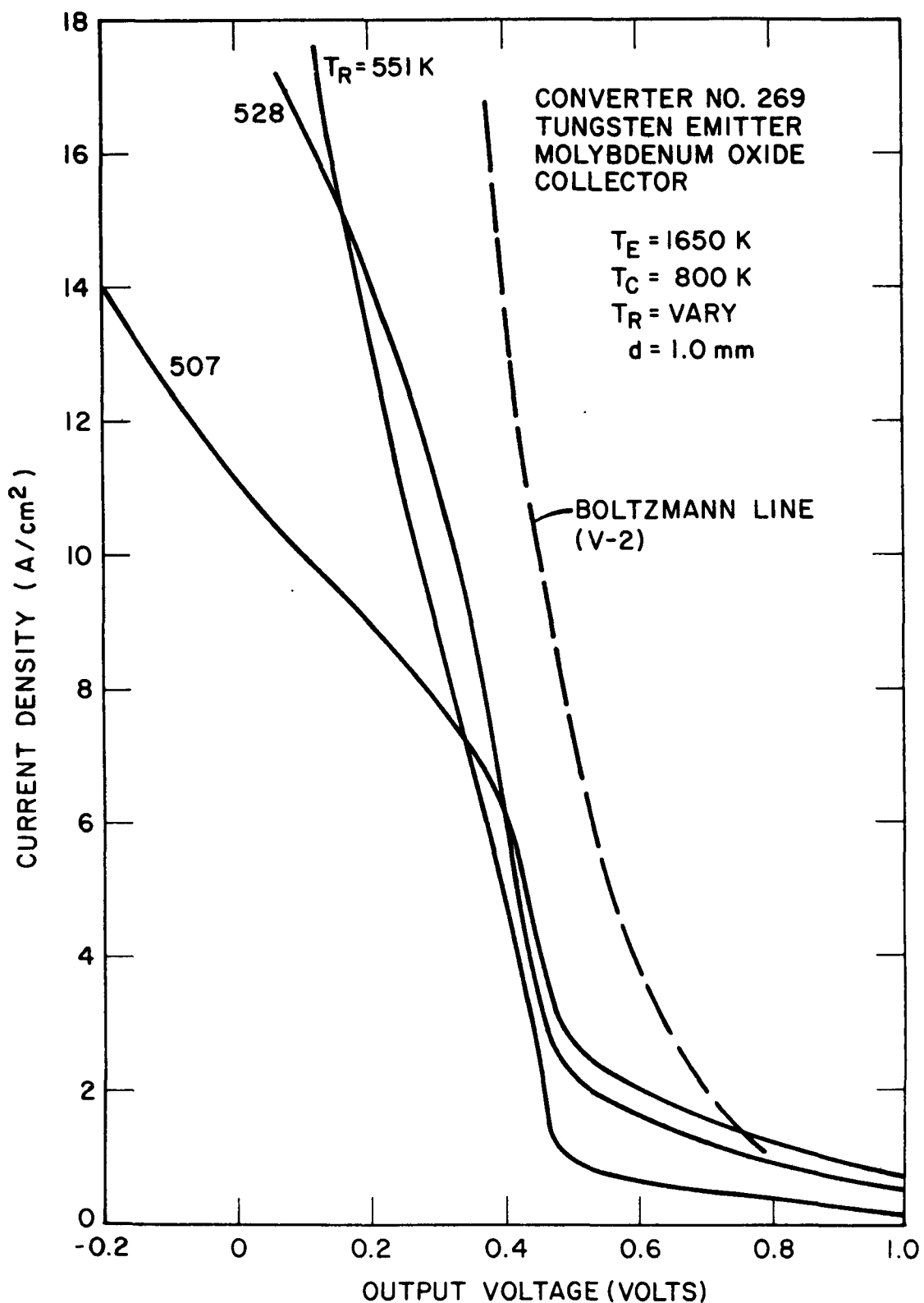


Figure 5. Cesium Reservoir Temperature Family at $T_E = 1650 \text{ K}$,
 $T_C = 800 \text{ K}$, and $d = 1.00 \text{ mm}$ for Converter No. 269

C. POSTOPERATIONAL ANALYSIS

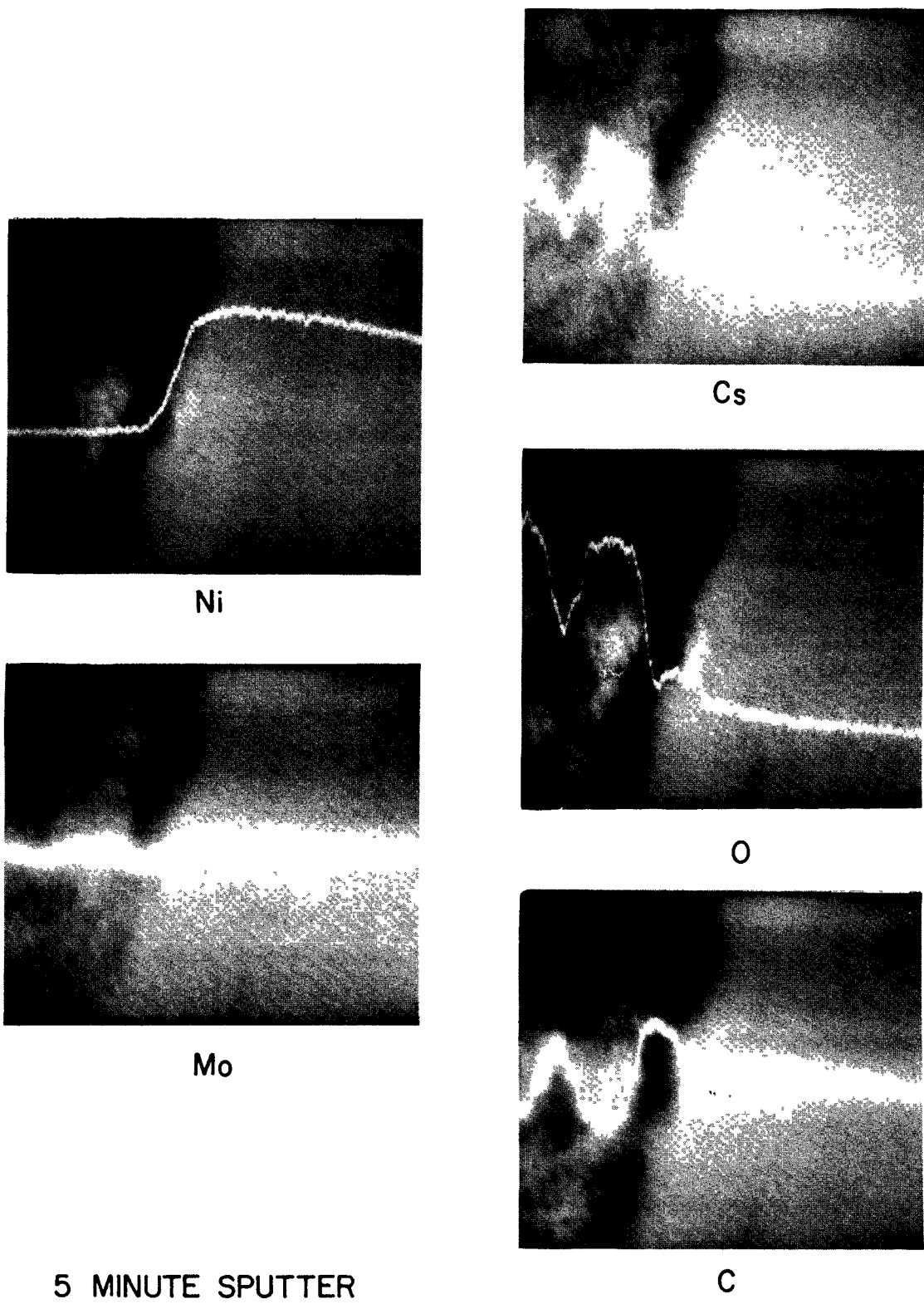
1. Converter No. 262: Tungsten Emitter, Sublimed Molybdenum Collector

Additional postoperational diagnoses were performed on the molybdenum-nickel interface region of the collector of Converter 262. In Progress Report 47, this region was analyzed with high resolution energy-dispersive spectroscopy for elements above mass number twelve. The sample was resubmitted to Photometrics for analysis by scanning Auger microscopy, which detects all elements above mass number two.

The Auger line scans for nickel, molybdenum, cesium, oxygen, and carbon after sputtering for five minutes are shown in Figure 6. The line scans are superimposed on an absorbed current micrograph of the interface region. The cesium, oxygen, and carbon profiles show peaks and valleys, indicating granular texture rather than uniform concentrations of those elements. A striking feature is the close correspondence between the oxygen and cesium profiles over the entire area surveyed.

Similar line scans after fourteen minutes of sputtering are shown in Figure 7. Again, the cesium and oxygen profiles coincide, indicating strong interaction between cesium and oxygen. Apparently, a cesium oxide is formed rather than molybdenum oxide plus cesium. The carbon profile is approximately the negative of the cesium and oxygen profiles, implying that carbon containing granules are distinct from the cesium oxide type granules.

A possible model emerges for the action of cesium during the operation of a converter with a sublimed molybdenum collector. The cesium penetrates into the bulk sublimed layer and reacts with the available oxygen to form a cesium oxide. This cesium oxide exists as granules rather than as a uniform distribution throughout the bulk. This filling of the bulk with cesium oxide may correspond with the "activation stage" of sublimed molybdenum collector converters. The molybdenum oxide is



5 MINUTE SPUTTER

Figure 6. Auger Line Scans Over Sublimed Molybdenum/Nickel Interface for Converter No. 262 After 5 Minutes of Sputtering

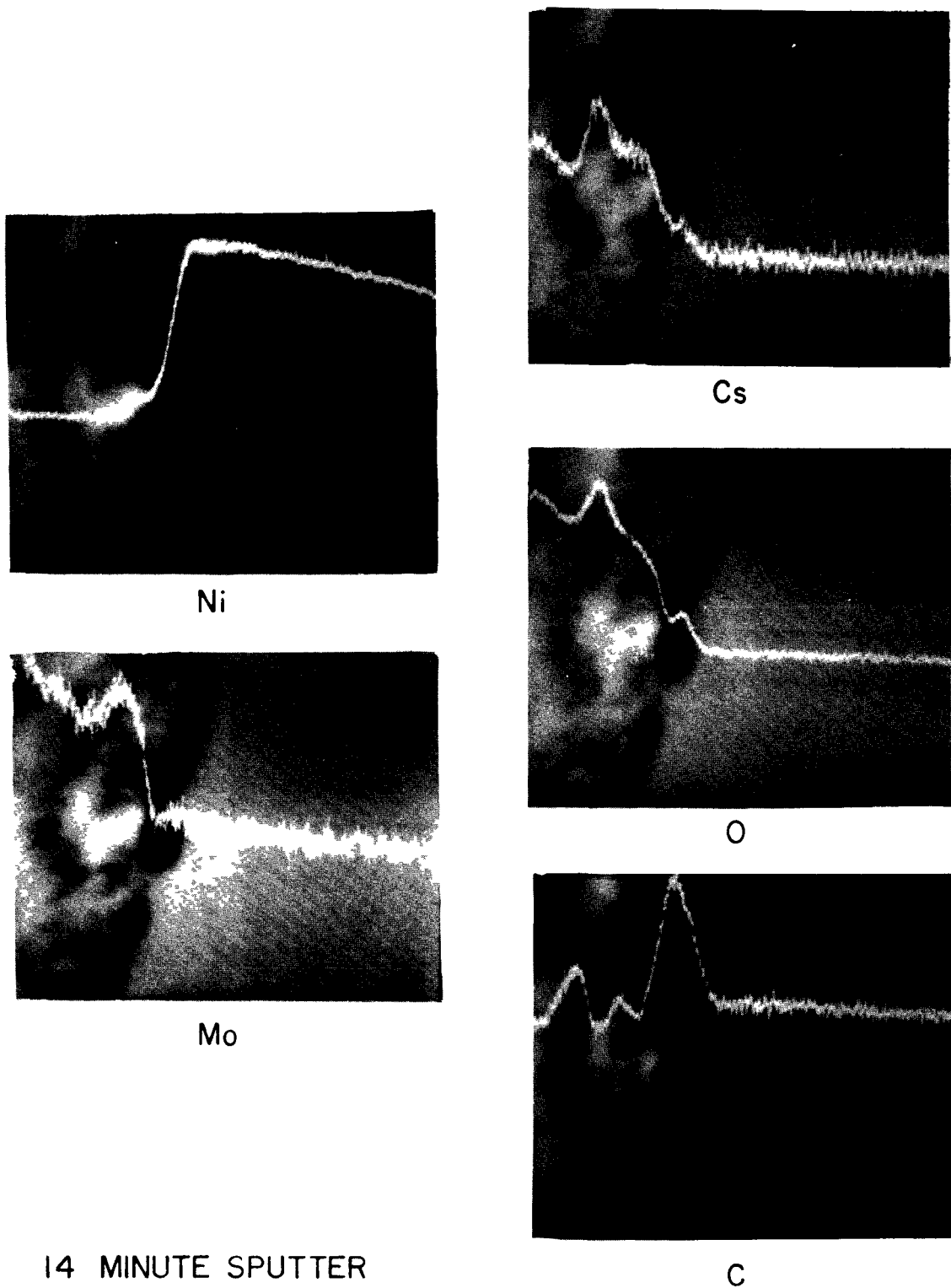


Figure 7. Auger Line Scans Over Sublimed Molybdenum/Nickel Interface for Converter No. 262 After 14 Minutes of Sputtering

then a reservoir of cesium oxide, and some cesium oxide desorbs to provide the "oxygen effect" seen at the emitter. This model ties in well with previous data³ which indicates that the "oxygen effect" is caused by cesium oxides.

The sputtered surface of the sublimed molybdenum collector of Converter No. 262 was analyzed by Auger Electron Spectroscopy (cf. Table 1). Only a very small carbon concentration is evident, in agreement with analyses of the sublimed molybdenum collectors of Converter Nos. 249 and 257.⁴ Heating to 1150 K for 7 minutes in vacuum removed all elements except molybdenum, oxygen and cesium. The cesium concentration is reduced only a small amount after this heating to 1150 K, implying either strong bonding of cesium to the molybdenum oxide substrate or a diffusion limited desorption process.

After the 1150 K heating, the FERP work function was measured as a function of cesium dose time (Figure 8). The work function passes through a minimum at 1.62 eV and then gradually increases. Since this cesium dosing technique covers the full range of cesium coverage expected in a converter, it may be possible to estimate the minimum operating collector work function by such a graph of FERP work function versus cesium dose.

2. Converter Nos. 261 and 268: DFVLR Electrodes

The emitters and collectors of Converter No. 261 (Emitter No. 1, Collector No. 1) and Converter No. 268 (Emitter No. 2, Collector No. 2) were analyzed by Auger electron spectroscopy. After operation, the emitters appeared uniformly gray with no obvious deposits. However, the collectors were covered with a black coating.

The postoperational Auger analysis results for the samples ("as admitted" and "sputtered") are given in Table 2. Collector No. 1 as admitted was sufficiently resistive that it was impossible to take an Auger

8111-60

TABLE 1
AUGER ELEMENTAL CONCENTRATIONS FOR THE COLLECTOR OF
CONVERTER NO. 262 AFTER SPUTTERING AND VACUUM ANNEAL

Element	Percent Concentration	
	After Sputtering	After Cs Dosing plus 1150 K Anneal
Mo	37.8	42.5
O	39.8	42.09
C	1.4	--
Cs	18.9	15.6
Cu	2.0	--

8110-23

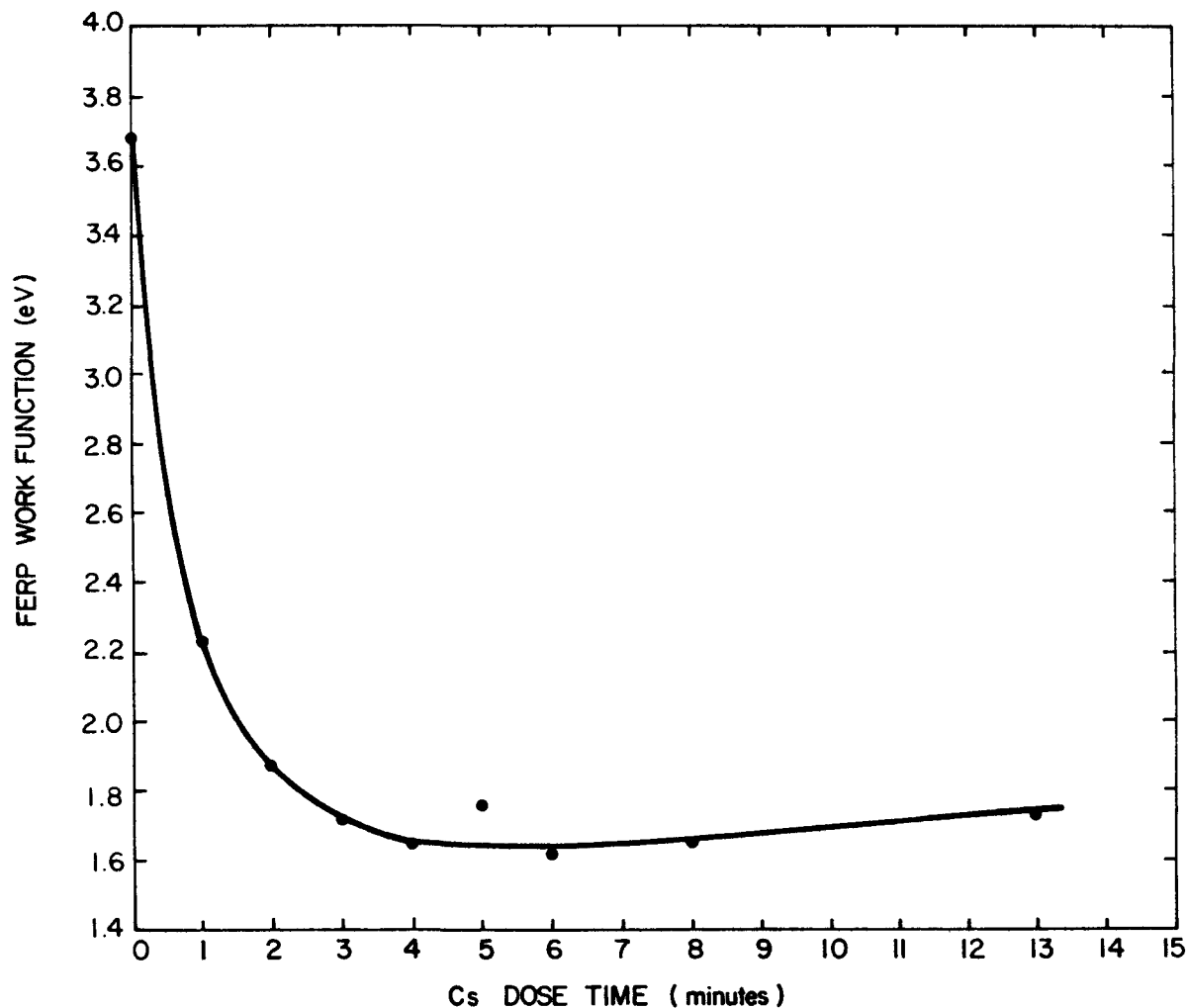


Figure 8. FERP Work Function vs Cesium Dose Time

TABLE 2
POSTOPERATIONAL AUGER ANALYSIS FOR ZrO_2/Mo
CERMET EMITTERS AND COLLECTORS

Element	As Admitted				After Sputtering			
	Collectors		Emitters		Collectors		Emitters	
	No. 1*	No. 2	No. 1	No. 2	No. 1	No. 2	No. 1	No. 2
Mo ₂₀₄₄		11.4	24.0	35.7	17.3	10.0	48.5	36.3
Zr ₁₈₄₅		--	14.3	18.4	--	--	14.8	15.2
O ₅₁₀		28.0	23.7	24.7	37.9	31.5	20.5	23.5
C ₂₇₃		3.2	14.6	7.1	2.3	2.5	14.2	23.5
N ₃₈₀		--	0.9	0.6	--	--	2.2	1.5
Cs ₅₆₃		10.8	22.5	13.3	7.3	5.7	--	--
Ca ₂₉₁		7.6	--	--	3.2	5.7	--	--
Si ₁₆₂₀		11.0	--	--	--	11.3	--	--
Ni ₈₄₈		1.6	--	--	1.4	3.6	--	--
Mg ₁₁₈₀		2.0	--	--	--	1.4	--	--
Al ₁₃₈₀		4.4	--	--	30.6	9.7	--	--
P ₁₈₅₉		20.0	--	--	--	18.6	--	--

*No Auger spectrum possible due to high resistivity of surface.

spectrum. Collector No. 2 was heavily oxidized with impurities of cesium, carbon, calcium, silicon, nickel, magnesium, aluminum and phosphorus. The as admitted emitters were free from all impurities except cesium, carbon and nitrogen.

The sputtered collectors still contained many impurities, including cesium. The presence of cesium indicates a bulk interaction between the oxide in the collector and cesium, similar to that in the sublimed molybdenum collectors. The emitters, by contrast, contained no cesium after sputtering - indicating only surface adsorption of cesium on the emitters.

A comparison of the elemental compositions of the sputtered electrodes before and after converter operation is given in Table 3. The collectors after operation show heavy oxidation and large impurity concentrations which obscure the molybdenum and zirconium signals. The impurities of calcium, silicon and nickel are apparently desorbed from the emitter onto the collector during converter operation.

The phosphorus, aluminum and magnesium impurities either diffuse from the bulk collector or are absorbed from the gas phase from an unknown source during converter operation. The carbon concentration on the collectors is greatly reduced after operation. This is similar to the small carbon concentrations found on sublimed molybdenum collectors and is apparently caused by carbon combining with the bulk oxygen and desorbing as CO or CO₂.

The emitter elemental concentrations are nearly equal before and after operation, except for the removal of some impurities. This result suggests stability of the emitter cermet material at high temperatures for short periods (1700 K, 10 hours for Converter No. 261 and 1600 K, 2 hours for Converter No. 268). The ZrO₂/Mo cermet electrodes thus look promising as permanently oxidized emitters providing that impurities can be prevented from depositing onto the collector.

TABLE 3
COMPARISON OF ELECTRODES BEFORE AND AFTER CONVERTER OPERATION
(ALL SURFACES SPUTTERED)

Element	Collectors				Emitters			
	No. 1 Before	No. 1 After	No. 2 Before	No. 2 After	No. 1 Before	No. 1 After	No. 2 Before	No. 2 After
Mo ₂₀₄₄	54.1	17.3	38.4	10.0	39.6	48.5	33.2	36.3
Zr ₁₈₄₅	4.9	--	7.7	--	10.1	14.8	9.2	15.2
O ₅₁₀	17.9	37.9	25.3	31.5	20.3	20.5	23.2	23.5
C ₂₇₃	17.9	2.3	17.3	2.5	22.9	14.2	24.6	23.5
N ₃₈₀	2.0	--	1.5	--	1.5	2.2	3.1	1.5
Ca ₂₉₁	0.9	3.2	3.2	5.7	1.9	--	1.7	--
Si ₁₆₂₀	2.0	--	5.3	11.3	2.8	--	4.0	--
Na ₉₉₆	--	--	0.3	--	--	--	0.5	--
Ni ₈₄₈	--	1.4	0.5	3.6	0.7	--	0.4	--
Fe ₇₀₃	--	--	0.4	--	--	--	--	--
Cs ₅₆₃	--	7.3	--	5.7	--	--	--	--
Mg ₁₁₈₀	--	--	--	1.4	--	--	--	--
Al ₁₃₈₀	--	30.6	--	9.7	--	--	--	--
P ₁₈₅₉	--	--	--	18.6	--	--	--	--

No. 1 refers to Converter No. 261; No. 2 refers to Converter No. 268.

II. COMBUSTION HEATED CONVERTER DEVELOPMENT

The objective of this task is to develop flame-fired thermionic converters that are as prototypic of projected terrestrial applications as possible. These converters will be constructed with CVD hot shell-emitter structures and designed to minimize expensive materials and construction techniques.

A. CONVERTER NO. 239: ONE-INCH DIAMETER HEMISPHERICAL SILICON CARBIDE CONVERTER (CVD TUNGSTEN AS DEPOSITED EMITTER, NICKEL COLLECTOR)

This converter continued on life test during this reporting period. The diode has accumulated 9800 hours of operating time at an emitter temperature of 1730 K. The dc output is 6 to 7 A/cm² at 0.3 V and is stable. This test is continuing.

B. CONVERTER NO. 266: TWO-INCH DIAMETER TORISPHERICAL SILICON CARBIDE CONVERTER (CVD TUNGSTEN AS DEPOSITED EMITTER, NICKEL COLLECTOR)

Converter No. 266 was installed in the multi-converter furnace and slowly heated to an emitter temperature of 1600 K. The initial performance measured during the heating period was encouraging. The barrier index at an emitter temperature at 1400 K was 2.15 eV. The slope of the I-V curve indicated there was no resistance problem in the diode. The emitter temperature was uniform over the entire surface, and the emitter-collector spacing was reasonable at the optimum operating temperatures.

However, after 20 hours of operation, the performance deteriorated rapidly. The converter output became unstable and appeared to have developed a leak. The diode was removed and leak checked. The ceramic seal that electrically insulates the electrodes had cracked and the diode leaked at this location. The converter was cut open and examined. The electrodes had become oxidized after the leak occurred. Construction of a new thermionic diode identical to Converter No. 266 will begin during the next reporting period.

**C. CONVERTER NO. 270: TWO-INCH DIAMETER TORISPHERICAL
SILICON CARBIDE CONVERTER (CVD TUNGSTEN AS DEPOSITED
EMITTER, SUBLIMED MOLYBDENUM COLLECTOR)**

A combustion heated converter with a sublimed molybdenum collector has been constructed. The hot shell-emitter structure is the standard two-inch torispherical configuration. The collector consists of an air-cooled nickel assembly with a 0.010-inch-thick coating of molybdenum sublimed in a low pressure of oxygen. The oxygen content of the coating is 13,000 ppm. The diode has been assembled and outgassed. Testing will begin during the next reporting period.

D. CVD SILICON CARBIDE COATING INSIDE SINTERED MOLYBDENUM TUBE

For another design concept of a flame-heated converter formulated by Rasor Associates, the configuration shown in Figure 9 is of interest. In this case, approximately 0.010 inch of silicon carbide was deposited on the inside of the molybdenum tube and 0.002 inch on the outside of the sintered molybdenum tube. No cracks or peeling were observed on the inside coating. The silicon carbide coated molybdenum tube was temperature cycled to 1500 K five times in vacuum with R.F. induction heating. No deterioration of the coating was observed on the silicon carbide coating after the temperature cycling.

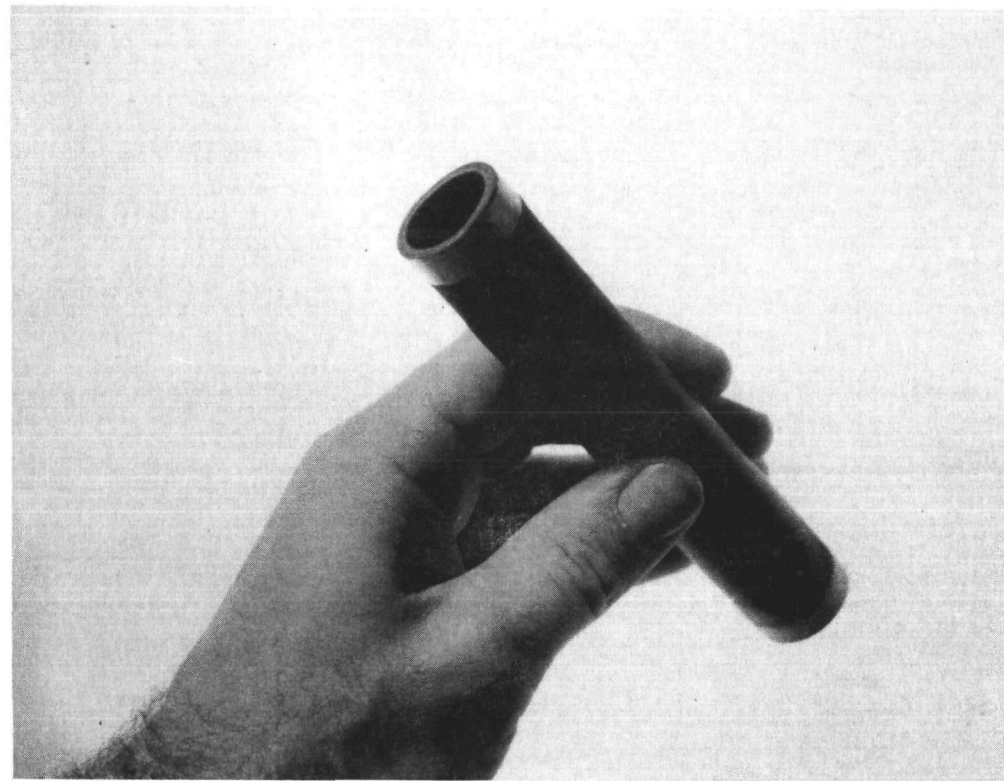


Figure 9. CVD SiC Coating Deposited Inside Sintered Molybdenum Tube

22

III. SYSTEM STUDIES

The objective of this task is to identify and evaluate systems utilizing thermionic energy conversion to improve efficiency and reduce cost. Both powerplant and high-temperature cogeneration processes will be considered.

An attractive application for the thermionic combustor is cogeneration with high-temperature processes. In order to illustrate the application of thermionic cogeneration, a case study of a steel slab reheat furnace is in progress. In such a furnace, steel slabs are heated to around 1475 K prior to being rolled in a mill. A walking beam reheat furnace manufactured by the Holcroft Division of Thermo Electron is shown in Figure 10. The reheat furnace and the associated rolling mill require a large amount of fuel and electricity.

Banks of burners are mounted on the sides of the furnace so that they fire above and below the slab. The flue gases from the furnace are ducted to the recuperator where the incoming combustion air for the burners is preheated. A drawing of the type of Bloom burners used on this furnace is shown in Figure 11.

The design concept of a thermionic combustor using a Bloom burner is illustrated in Figure 12. The thermionic converters are similar to those described in Chapter II of this report. The air for cooling the collectors of the converters is split into two streams. One stream provides combustion air and the other stream is used to dilute the combustion gases to the temperature desired for the process. A flow diagram for the thermionic combustor is given in Figure 13.

Based on this flow diagram, a computer program has been written to calculate the characteristics and performance of the thermionic combustor. A flow chart of this program is shown in Figure 14.

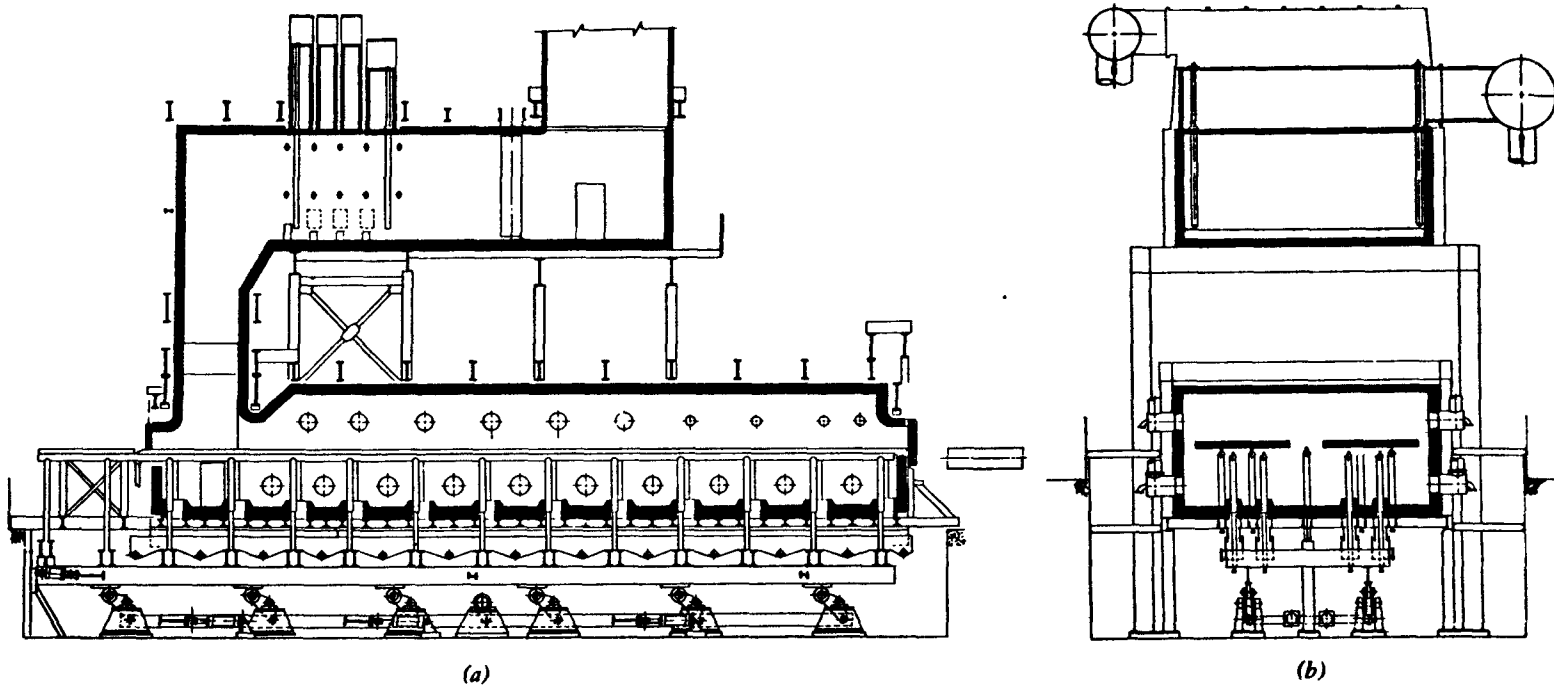
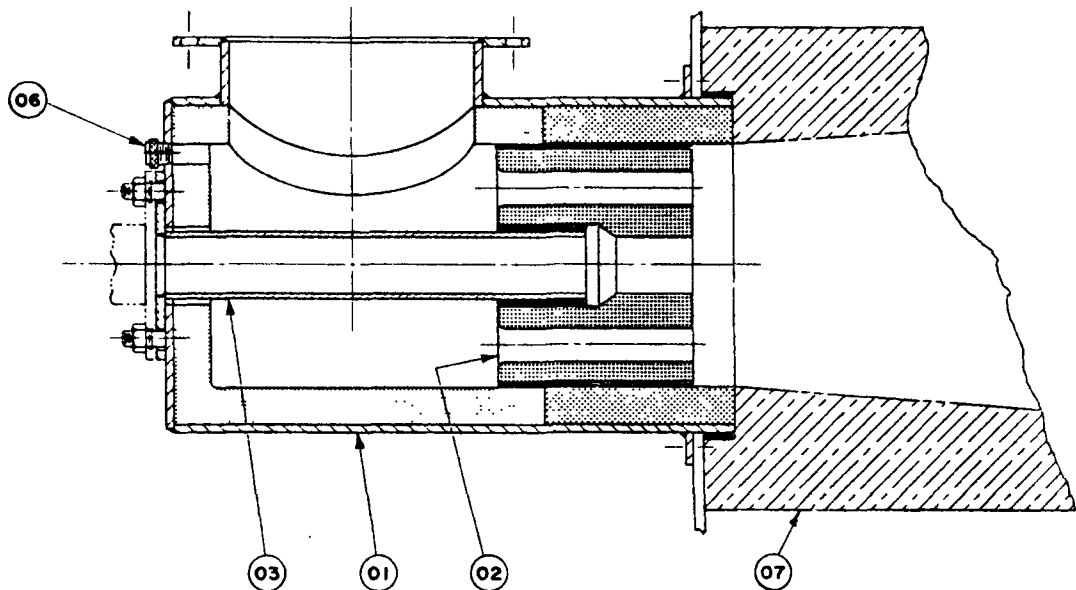


Figure 10. Water-Cooled Rail System in Walking Beam Furnace: (a) Longitudinal Section, (b) Cross Section



Part Number	Description
01	Body
02	Baffle
03	Nozzle Assembly
06	Observation Port
07	Port Block

Figure 11. Bloom Burner Used on Holcroft Reheat Furnace

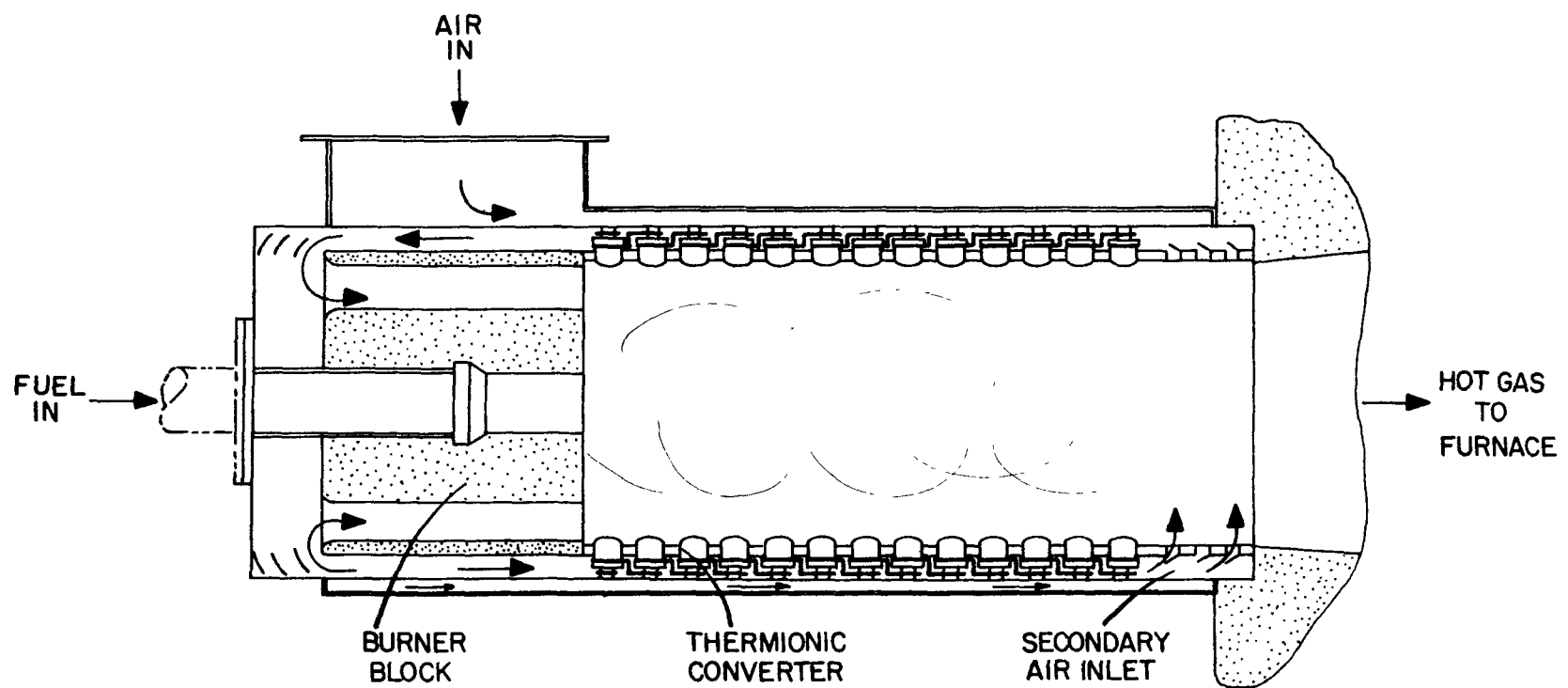


Figure 12. Design Concept of Thermionic Combustor Using a Bloom Burner

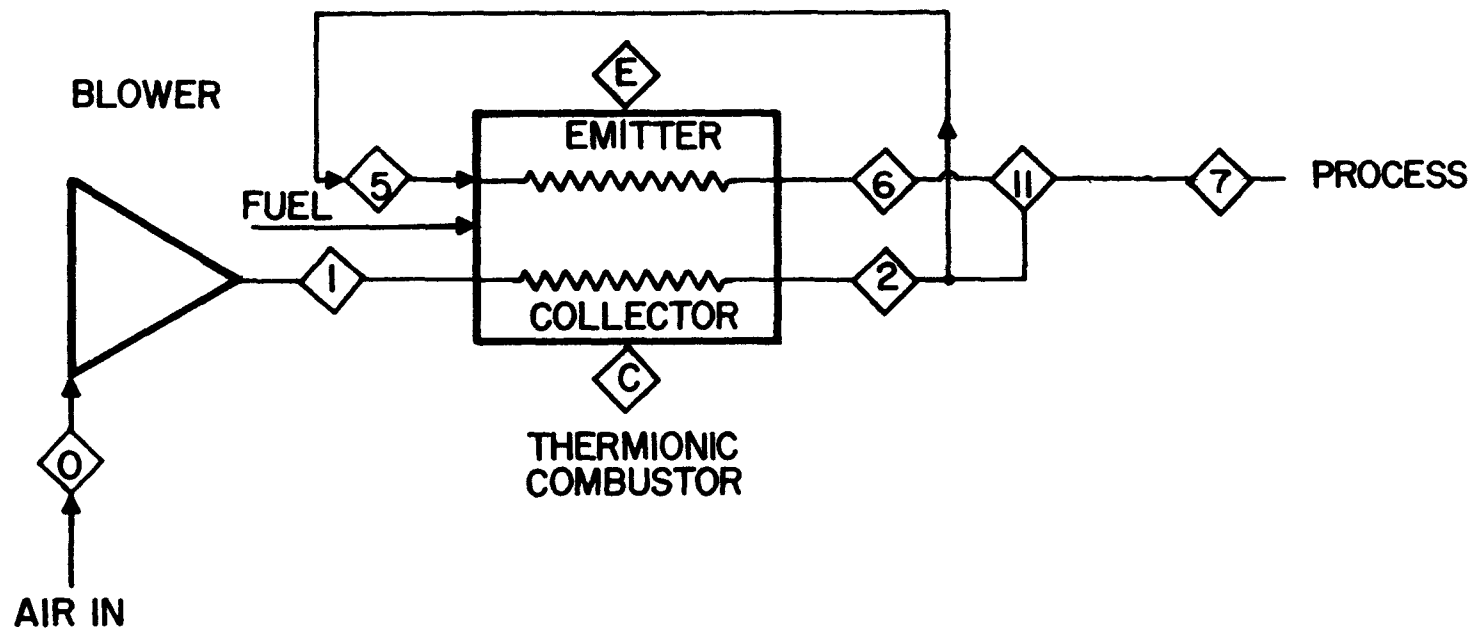


Figure 13. Flow Diagram for Thermionic Combustor

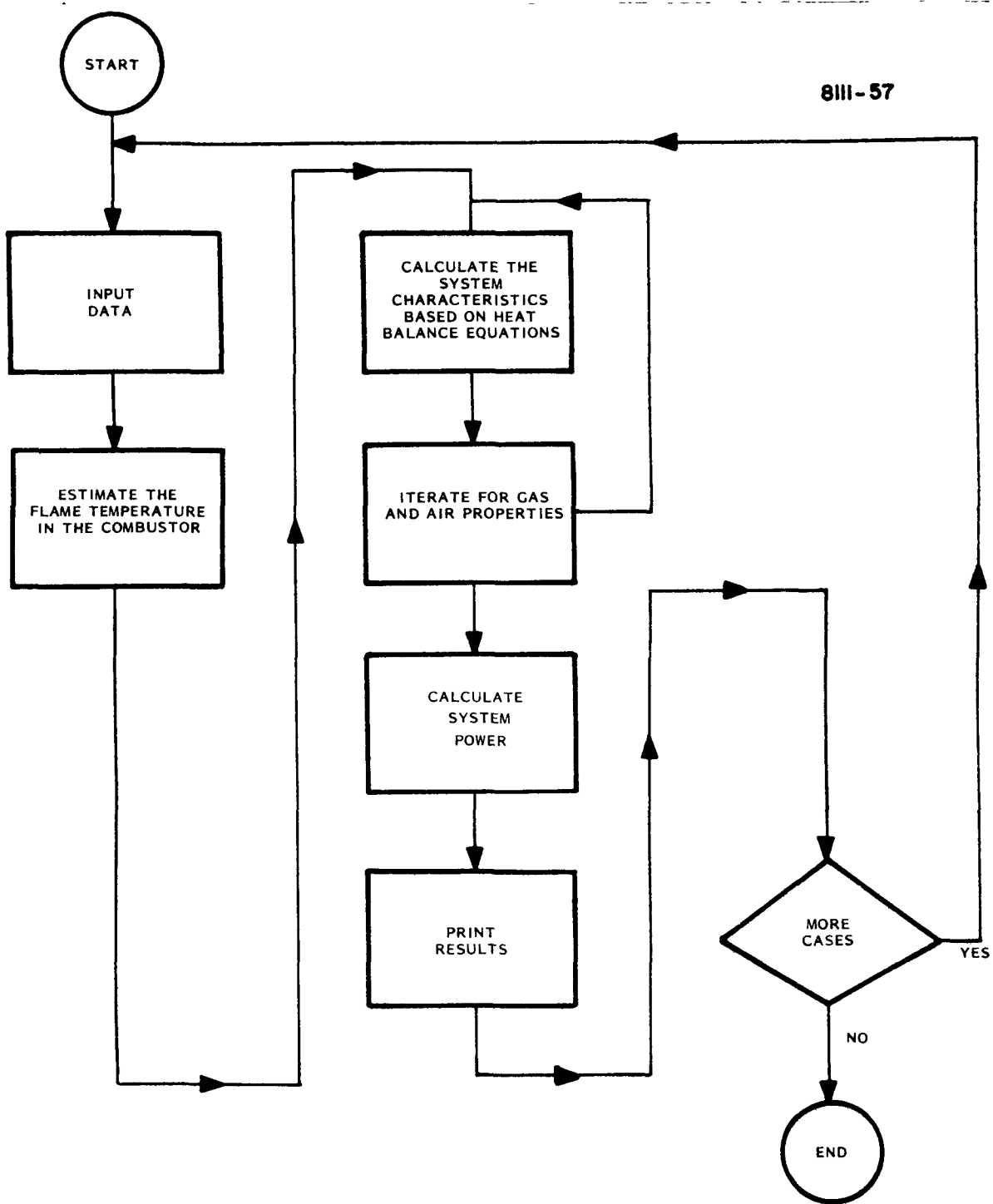


Figure 14. Flow Chart of Thermionic Combustor Program

IV. CONVERTER PRODUCTION ENGINEERING

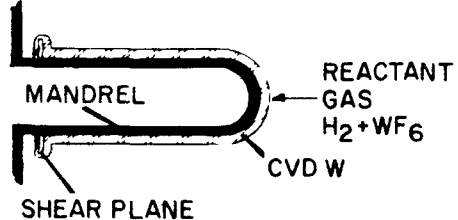
The objective of this task is to develop techniques suitable for high-volume production rates which will require automation of assembly and processing steps as well as a modified CVD fabrication method.

Two methods of fabricating low cost hot shell-emitter structures are being investigated which eliminate the nonreusable graphite mandrel. In both methods, a thin carbon coating is substituted in place of the graphite shell. The primary difference between the methods is the order of deposition of silicon carbide and tungsten. The two procedures are illustrated in Figure 15. During this reporting period, most of the work concerned Method A.

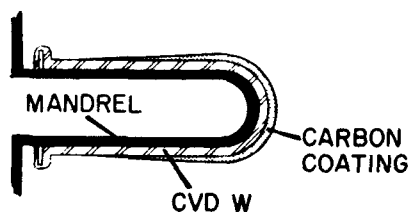
Previously, two leaktight hot shell-emitter structures were produced by Method A. Their configuration duplicated that of the two-inch tori-spherical hot shell-emitter structure that has been successfully made by starting with a graphite mandrel. After copper brazing the first shell to a molybdenum flange, the silicon carbide cracked at the base of the shell. The second shell remained leaktight after the braze cycle and was set up to be R.F. heated in air. A nickel flange and tube were electron beam welded to the molybdenum flange and attached to a small diffusion pump to monitor the pressure during the testing. During the first heating cycle, the silicon carbide cracked at the base of the shell. The location of the crack and the area of a silicon carbide flake from the shell are shown in Figure 16. The tungsten coating remained leaktight during this first temperature cycle to 1400 K.

No further shells were made by Method A because of the low yield of leaktight tungsten shells produced in the first step. During deposition of tungsten or during cool-down, the shell would usually crack. This event was observed via a sight port located at the input flange of the Lindberg furnace. A photograph of the two cracked, free-standing tungsten shells is shown in Figure 17. Since there was a low success rate using Method A, the effort during the next reporting period will be concentrated on Method B.

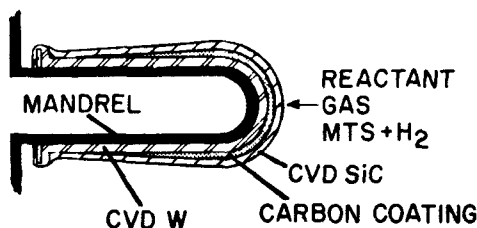
30



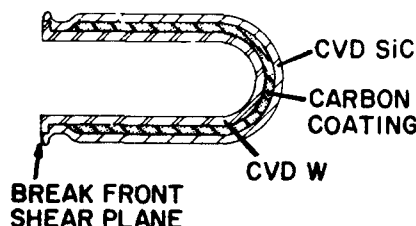
CVD
TUNGSTEN
EMITTER



CARBON
COATING

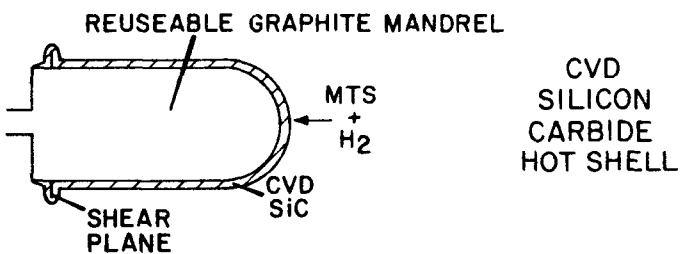


CVD
SILICON
CARBIDE
HOT SHELL

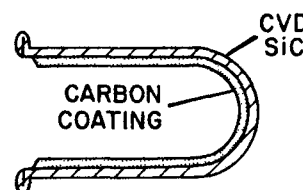


COMPOSITE
HOT SHELL/
EMITTER

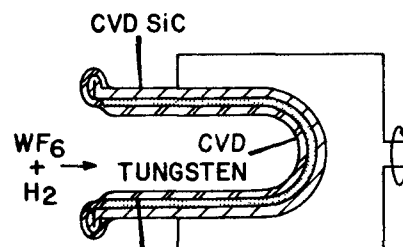
METHOD A



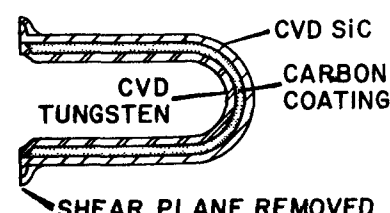
CVD
SILICON
CARBIDE
HOT SHELL



CARBON
COATING



CVD
TUNGSTEN
EMITTER



COMPOSITE
HOT SHELL/
EMITTER

METHOD B

Figure 15. Fabrication Techniques for Production

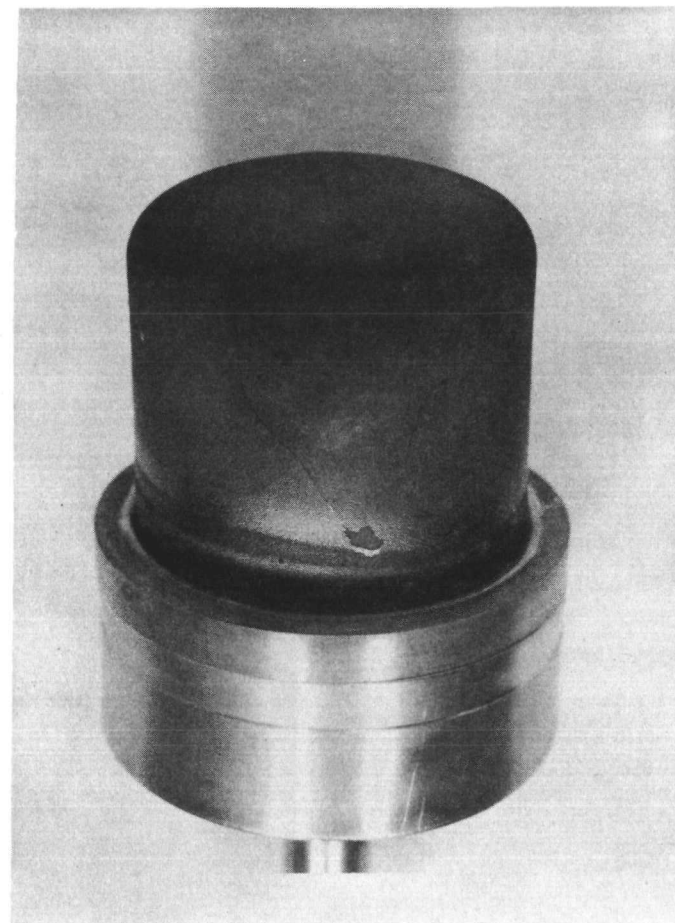


Figure 16. Hot Shell-Emitter Structure Fabricated by Method A After Flange Braze. Note Crack and Flaked Area.

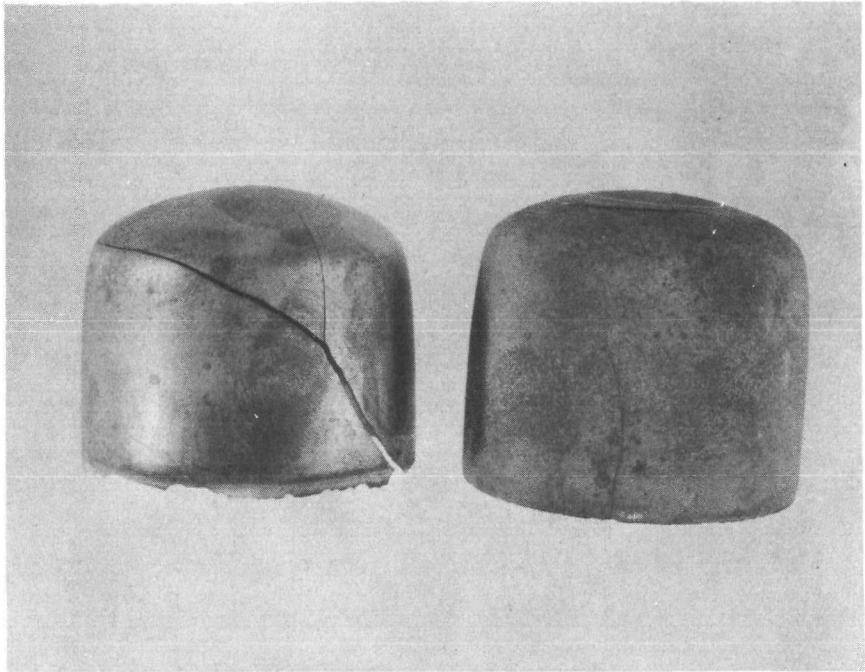


Figure 17. Cracked Tungsten Shells Made Using Method A.

V. REFERENCES

1. M. Bradke and R. Henne, "State of Cermet Electrode Development for Flame Heated Thermionic Converters," Proc. 14th IECEC Conf., p. 1904 (1979).
2. R. Henne, M. Bradke and W. Weber, "Progress in the Development of Small Flame Heated Thermionic Energy Converters," Proc. 15th IECEC Conf., p. 2089 (1980).
3. M. Saunders, L.R. Danielson, and F.N. Huffman, "Investigations into the Mechanism of Operation of Thermionic Converters with Molybdenum Oxide Collectors," 1981 IEEE Int. Conf. on Plasma Science, Sante Fe, NM.
4. Thermo Electron Progress Report No. 46, TE4258-247-81, Thermo Electron Corporation, 1981.